

12,14,16

## Study of the mechanical properties of polystyrene during indentation by Mandelstam–Brillouin spectroscopy

© S.A. Votyakov<sup>1</sup>, I.A. Kudryashov<sup>2</sup>, C. Budich<sup>2</sup>, A.S. Useinov<sup>1</sup>, G.Kh. Sultanova<sup>1</sup>, I.V. Laktionov<sup>1</sup>

<sup>1</sup> Advanced Scientific Devices, LLC,  
Troitsk, Moscow, Russia

<sup>2</sup> Tokyo Instruments,  
Tokyo, Japan

E-mail: savotyakov99@yandex.ru

Received November 28, 2024

Revised December 28, 2024

Accepted December 31, 2024

The transparent diamond indenter lens is effective when used with Raman spectrometers. However, there are polymer samples, in particular polystyrene, that are weakly sensitive to this type of spectroscopy, but sensitive to Mandelstam–Brillouin spectroscopy. In this regard, the point process of studying the deformation of the polystyrene material is relevant both during *in situ* loading and after removing the load. Similar experimental conditions without the use of special immersion liquids can be achieved by a combined system of the transparent diamond indenter lens, combined with a confocal Brillouin microscope in a backscattered light configuration. The areas under the imprint and beyond it during indentation under the load of 1 N and after loading the material were estimated pointwise by the frequency shifts of the Brillouin spectra of the polystyrene sample.

**Keywords:** transparent indenter, Mandelstam–Brillouin spectroscopy, indentation.

DOI: 10.61011/PSS.2025.01.60602.355

### 1. Introduction

The transparent diamond indenter lens is effective when used with Raman spectrometers and allows studying samples during indentation *in situ* without using special immersion fluids and studying the mechanical properties of materials in a pointwise manner by combining mechanical tests with spectroscopic methods [1–3]. Phase transitions occurring during the deformation of crystalline materials and medicinal polymorphic modifications can be studied using Raman spectroscopy [4–5]. It is also possible to pinpoint and quantify stress values and their nature (tension or compression) both in the area under the indenter and beyond it, owing to the Grüneisen phonon mode tensor concept [6].

However, there are polymer samples, in particular polystyrene, that are weakly sensitive to Raman scattering spectroscopy, but at the same time provide a good signal from acoustic phonon vibrations. The Mandelstam–Brillouin spectroscopy method [7] is promising for such samples. This technique offers an optical method for studying the elastic and viscoelastic properties of polymers at acoustic phonon frequencies.

Polymer materials have recently been actively used in various fields of industrial production: in aviation, space technology, and laser technology. They are used to create nanocomposites with a polymer matrix [8], and to create dielectric optical microresonators [9]. Polystyrene has become particularly widespread in the microresonator,

from which one-dimensional nanomaterials are integrated onto microspheres to create exciton generation [10]. The deposition of nanomaterials on the resonator causes the deformation of polystyrene, which can prevent generation because of changes of the geometric properties of the resonator.

It is important to study in detail the mechanical properties of polystyrene both during loading *in situ* and after removing the load. In particular, this can help optimize the methods of deposition of nanomaterials on polymers. The comprehensive deformation is simulated using an indenter. The nature of the deformed regions is determined by the shear characteristics of the Stokes component, and the predominance of individual deformation components in different areas under the indenter is estimated. This paper demonstrates the possibility of point mapping of deformed regions under the indenter and beyond using Brillouin frequency shifts. Comparing the data of the loaded sample maps and the sample maps after removing the load allows obtaining expanded information about the mechanical properties of the material. The extended capabilities of an indenter lens combined with a confocal Brillouin microscope are demonstrated.

### 2. Experimental methodology and theory

The Brillouin spectra are recorded under an indenter lens in the backscattering geometry. The Brillouin frequency

shift can be represented as follows in the backscattering configuration in an isotropic medium [11]:

$$\delta\nu_B = \frac{2n\nu_L}{\lambda_0}, \quad (1)$$

$$\nu_L = \sqrt{\frac{M}{\rho}},$$

where  $\rho$  is the density of the medium,  $n$  is the refractive index,  $\nu_L$  is the longitudinal velocity of sound in the medium,  $M$  is the longitudinal modulus of elasticity.

The parameters of the medium under load can vary greatly in areas of plastic deformation; they also slightly change in case of elastic deformations. An accurate quantitative calculation of changes in the density of the medium, the speed of sound and the longitudinal modulus of elasticity within the framework of this method remains difficult, since the variation of these parameters is interdependent. However, qualitative conclusions can be drawn about deformations and changes of the density of materials in the indentation area and beyond it when mapping the distribution of Brillouin frequency shifts. As in the case of Raman spectroscopy, the nature of the deformation, i.e. stretching or compression, is determined depending on the shift of peaks towards low or high frequencies, respectively. Frequency shift mapping is the most reliable, since it can be seen from the formula (1) that this shift includes all structural changes.

The areas under and outside the tip are subject to plastic and elastic deformations, but it is impossible to tell which of these types of deformation prevails at a particular point solely by frequency shifts, since peak displacement also occurs with exceptionally elastic deformation. This problem can be solved by comparing the same areas of the frequency shift distribution maps obtained during loading and after removing the load. If there are no frequency shifts in a certain area after the load is removed, whereas they were observed during loading, then this area is characterized by an elastic type of deformation during loading.

Combined system NanoScan® (Russia) with a confocal Brillouin microscope Nanofinder® (Tokyo Instruments, Inc.) was used in the experiment. The Brillouin system Nanofinder® included 532 nm laser (the radiation power at entrance of the transparent indenter is 6 mW), Flex2 confocal module, and a special „free space“ microscope with a base that allows the nanoindenter module to be placed under it. XYZ piezoscanner of the microscope lens was used for the precise positioning of the laser spot on the sample and mapping. The ability to quickly obtain high-quality spectra from each point allows studying the process of changing of mechanical characteristics when the loading parameters change.

A piece of transparent polystyrene with a density of 1.06 g/cm<sup>3</sup>, a refractive index of 1.6 and a Poisson's ratio of 0.34 was selected as the sample. The sample was secured using Crystalbond555 glue on a standard brass holder.

The basic mapping data were obtained at a load of 1 N. The scan area of 12 × 12 points included areas both inside and outside the indentation. The spectrum measurement time was 1 s per point in increments of 15 μm. When examining the residual indentation of the area of 80 × 60 points, the exposure time was 500 ms per point in increments of 2.5 μm. The Brillouin spectra were processed using an approximation of the Lorentz curve.

### 3. Results and their discussion

The areas of plastic and elastic deformation are studied under loading. The mapping is conducted using frequencies located at the maximum of the Stokes peak. The exact values are obtained by Lorentz approximation with a good signal-to-noise ratio. The conventional nonlinear least

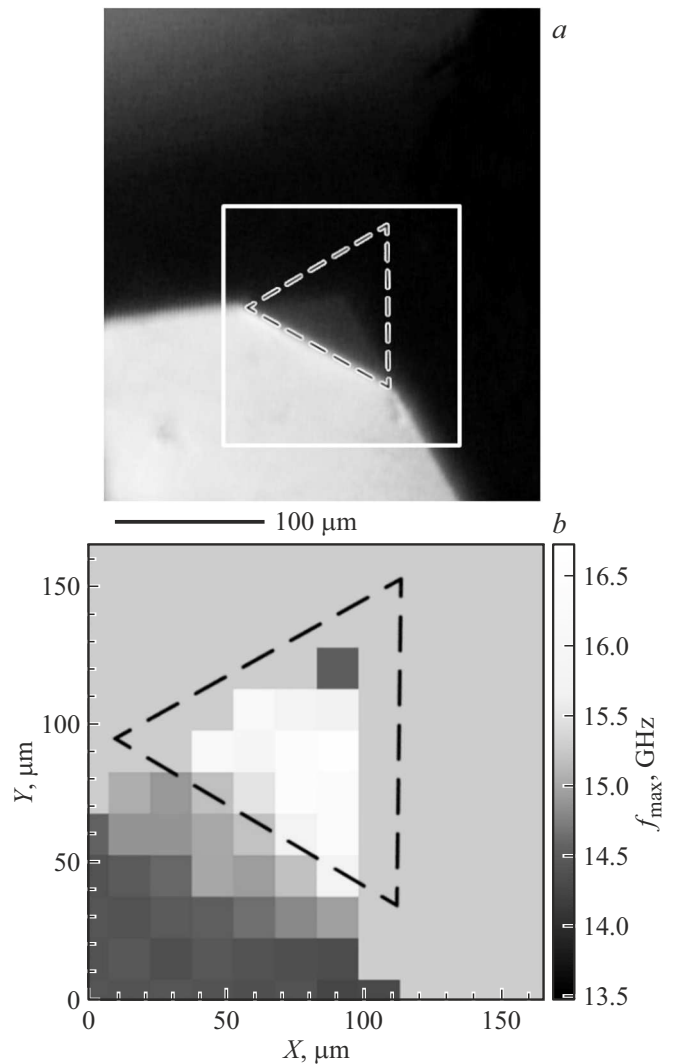


**Figure 1.** a) Microscopic image of the right segment of the indenter under load of 1 N. b) Point mapping of the right segment of the selected area based on shifts of peak values of the Brillouin spectra.  $f_{\max}$  — the frequency at which the maximum intensity of the Stokes peak is observed.

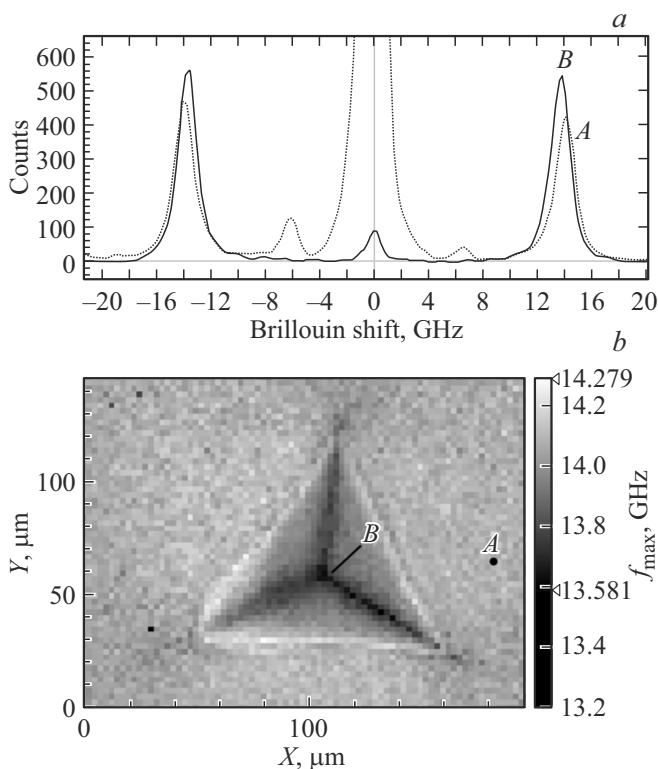


**Figure 2.** *a)* Brillouin spectra of the non-deformed region A and the tension deformation region B — the low-frequency region of the residual indentation in the center. *b)* Point mapping of the residual indentation based on shifts of peak values of the Brillouin spectra.

squares algorithm was used. The error in the approximation of the spectra was about 3%.

The scanning of the right segment of the indenter with a large step, both in the area under the tip and beyond, during indentation is performed for a preliminary assessment of the prevalent types of deformations. It can be seen from Figure 1, *b* that a shift occurs under the tip at the measured points to the high frequency range of about 16.5 GHz, which corresponds to a plastic deformation of strong compression. The black area corresponds to the area that is inaccessible for measurements within the current segment of the indenter (it is accessible for measurements through other segments), the dotted triangle corresponds to the area of the indentation. A shift to the high frequency range in the region of 15 GHz occurs at the measured points located outside the indentation, but it is impossible to determine based on these measurements whether the deformation profile corresponds to the elastic deflection profile, since plastic deformations may also occur outside the indentation. This can be understood by a pointwise detailed examination of the residual indentation with a small step: if the frequencies do not shift beyond the boundary of the residual indentation, then this profile can be considered an elastic deflection profile.

Figure 2, *b* shows Brillouin frequency mapping of the polystyrene residual indentation, including all segments of the indenter. Peaks tend to shift in the low frequency region in the regions under the tip, which indicates a tension deformation, whereas compressive deformation prevailed during indentation under the indenter. This change is attributable to the softening of the sample after loading. The frequency distribution shows that the greatest tension deformations prevail in the center and at the boundaries separating the indenter segments. Compression deformations prevail at the boundaries of the indentation itself, where the maximum of the spectra lies in the region of 14.3 GHz. This material has a uniform distribution of deformation. There are no gradient fields outside the indentation beyond its boundaries, from which it can be concluded that only the areas of application of the load are subjected to plastic deformation, and during indentation, an elastic deflection profile appears outside the indentation.

## 4. Conclusion

Frequency mapping has shown the effectiveness of the Mandelstam-Brillouin spectroscopy method in combination with instrumental indentation and in situ measurements. Obtaining high-quality spectra with a short exposure time for each point makes it possible to study in detail the nature of deformations in the sample.

Polystyrene materials tend to have tension deformations under the tip after application of a load, which indicates the softening of these samples after loading. At the same time, no residual plastic deformations were detected outside the indentation; therefore, the profile of deformations occurring outside the indentation during the application of the load corresponds to the profile of elastic deflection.

Such research methods become possible due to the expanded capabilities of usage of a transparent diamond indenter lens for instrumental indentation combined with Brillouin spectroscopy.

The study was performed using combined system NanoScan (Russia) / Nanofinder (Tokyo Instruments Inc., Japan).

## Conflict of interest

The authors declare that they have no conflict of interest.

## References

- [1] A. Useinov, V. Reshetov, A. Gusev, E. Gladkih. *J. Appl. Phys.* **132**, 12, 121101 (2022). <https://doi.org/10.1063/5.0099166>
- [2] I.I. Maslenikov, V.N. Reshetov, A.S. Useinov, M.A. Doronin. *Instrum. Exp. Tech.* **61**, 5, 719 (2018). <https://doi.org/10.1134/S002044121804022X>
- [3] I.I. Maslenikov, V.N. Reshetov, A.S. Useinov. *Mater. Trans.* **60**, 8, 1433 (2019). <https://doi.org/10.2320/matertrans.MD201902>

- [4] I.I. Maslenikov, A.S. Useinov. IOP Conf. Ser.: Mater. Sci. Eng. **699**, 1, 012027 (2019).  
<https://doi.org/10.1088/1757-899X/699/1/012027>
- [5] P. Manimunda, S.A.S. Asif, M.K. Mishra. Chemical Commun. **55**, 62, 9200 (2019). <https://doi.org/10.1039/C9CC04538D>
- [6] R.J. Angel, M. Murri, B. Mihailova, M. Alvaro. Z. f. Krist. Cryst. Mater. **234**, 2, 129 (2018).  
<https://doi.org/10.1515/zkri-2018-2112>
- [7] D. Rouxel, C. Thevenot, V.S. Nguyen, B. Vincent. In: Spectroscopy of Polymer Nanocomposites / Eds S. Thomas, D. Rouxel, D. Ponnammma. Ch. 2, pp. 362–392 (2016).  
<https://doi.org/10.1016/B978-0-323-40183-8.00012-4>
- [8] H.V. Rusakova, L.S. Fomenko, S.V. Lubenets, V.D. Natsik. Low Temperature Phys. **45**, 12, 1301 (2019).  
<https://doi.org/10.1063/10.0000213>
- [9] S. Liu, S. Tie, J. Chen, G. Li, J. Yang, S. Lan. Nanophotonics **11**, 21, 4715 (2022).  
<https://doi.org/10.1515/nanoph-2022-0380>
- [10] J.-S. Chen, A. Dasgupta, D.J. Morrow, R. Emmanuele, T.J. Marks, M.S. Hersam, X. Ma. ACS Nano **16**, 10, 16776 (2022). <https://doi.org/10.1021/acsnano.2c06419>
- [11] H. Tran, S. Clement, R. Violla, D. Vandembroucq, B. Ruffle. Appl. Phys. Lett. **100**, 23, 231901 (2012).  
<https://doi.org/10.1063/1.4725488>

*Translated by A.Akhtyamov*